Open Mathematics

Research Article

Nauman Ahmed*, Tahira S.S., M. Rafiq, M.A. Rehman, Mubasher Ali, and M.O. Ahmad

Positivity preserving operator splitting nonstandard finite difference methods for SEIR reaction diffusion model

https://doi.org/10.1515/math-2019-0027
Received July 15, 2018; accepted February 14, 2019

Abstract: In this work, we will introduce two novel positivity preserving operator splitting nonstandard finite difference (NSFD) schemes for the numerical solution of SEIR reaction diffusion epidemic model. In epidemic model of infection diseases, positivity is an important property of the continuous system because negative value of a subpopulation is meaningless. The proposed operator splitting NSFD schemes are dynamically consistent with the solution of the continuous model. First scheme is conditionally stable while second operator splitting scheme is unconditionally stable. The stability of the diffusive SEIR model is also verified numerically with the help of Routh-Hurwitz stability condition. Bifurcation value of transmission coefficient is also carried out with and without diffusion. The proposed operator splitting NSFD schemes are compared with the well-known operator splitting finite difference (FD) schemes.

Keywords: SEIR reaction diffusion model, operator splitting techniques, positivity, bifurcation value.

1 Introduction

In childhood epidemic diseases, Measles is considered as highly infectious disease, spread due to respiratory infection by a traveling virus. In 19th century, Arthur Ransom observed the unevenly recurring nature of Measles. Since 1896, age structures, contact rates and school seasons are known as critical agents for the transmission of Measles in a population. Hamer [1] in 1906 presented a model for transmission dynamics of Measles. Later, the principle of "mass action" was introduced which became a fundamental statute in present theory of infectious disease modeling [2–5].

Infectious disease dynamics is an important application of dynamical systems. Fixed points, steady states or the equilibrium points of a continuous dynamical systems are the values of variables that do not change over time. If a system starts at a nearby state and converges to the equilibrium point, then this equilibrium point is attractive. Many dynamical systems in different fields of science and engineering show the chaotic behavior.

***Corresponding Author: Nauman Ahmed:** Department of Mathematics, University of Management and Technology, Lahore, Pakistan, E-mail: nauman.ahmd01@gmail.com
Tahira S.S.: Department of Mathematics, Lahore College for Women University, Lahore, Pakistan, E-mail: tahira.sumbal@lcwu.edu.pk
M. Rafiq: Faculty of Engineering, University of Central Punjab, Lahore, Pakistan, E-mail: m.rafiq@ucp.edu.pk
M.A. Rehman: Department of Mathematics, University of Management and Technology, Lahore, Pakistan, E-mail: aziz.rehman@umt.edu.pk
Mubasher Ali: Department of Electrical Engineering, University of Lahore, Lahore, Pakistan, E-mail: mubasherali4@gmail.com
M.O. Ahmad: Department of Mathematics and Statistics, University of Lahore, Lahore, Pakistan, E-mail: drchadury@yahoo.com

If a numerical method produces chaos and it is not the feature of continuous system, then this is called contrived chaos. Many existing numerical techniques show the contrived chaos. If a continuous dynamical system demonstrates a property P, then it is necessary for the numerical method to preserve that property P. This is called dynamical consistency, in the literature, Twizzell et al and various authors [6–13] discussed about the contrived chaos and loss of the dynamical consistency in the finite difference scheme. Similarly, Fernández [14] discussed about the same drawbacks exhibited in different series solution techniques. The aim of this work is to develop and investigate such numerical schemes whose equilibrium points coincide with the equilibrium points of the continuous system and preserve all the essential properties demonstrated by the continuous system.

In this work, we consider SEIR epidemic model with diffusion presented by Al-Shawaikh and Twizell [15]. This model describes the transmission dynamics of measles. In this model, the total population is taken as 'N' and it is categorized in four classes i.e. susceptible population, exposed population, infected population and recovered population denoted by S, E, I and R respectively. It is assumed that the total population 'N' is constant i.e. birth and death rates in the population are equal. Mathematical model of SEIR epidemic model with diffusion is

$$\frac{\partial S}{\partial t} = \mu N - \mu S - \beta SI + d_S \frac{\partial^2 S}{\partial x^2}, \tag{1}$$

$$\frac{\partial E}{\partial t} = \beta SI - (\mu + \sigma) E + d_E \frac{\partial^2 E}{\partial x^2}, \tag{2}$$

$$\frac{\partial I}{\partial t} = \sigma E - (\mu + \gamma) I + d_I \frac{\partial^2 I}{\partial x^2}, \tag{3}$$

$$\frac{\partial R}{\partial t} = \gamma I - \mu R + d_R \frac{\partial^2 R}{\partial x^2}. \tag{4}$$

Since R is not present in first three equations so we can write the system as

$$\frac{\partial S}{\partial t} = \mu N - \mu S - \beta SI + d_S \frac{\partial^2 S}{\partial x^2}, \tag{5}$$

$$\frac{\partial E}{\partial t} = \beta SI - (\mu + \sigma) E + d_E \frac{\partial^2 E}{\partial x^2}, \tag{6}$$

$$\frac{\partial I}{\partial t} = \sigma E - (\mu + \gamma) I + d_I \frac{\partial^2 I}{\partial x^2}, \tag{7}$$

with the initial conditions

$$S(x, 0) = g_1(x), E(x, 0) = g_2(x), I(x, 0) = g_3(x), 0 \le x \le L \tag{8}$$

and homogeneous Neumann boundary conditions are

$$S_x(0, t) = S_x(L, t) = 0, \tag{9}$$

$$E_x(0, t) = E_x(L, t) = 0, \tag{10}$$

$$I_x(0, t) = I_x(L, t) = 0. \tag{11}$$

As discussed above, the purpose of this work is to construct positivity preserving operator splitting non-standard finite difference schemes for the system (5)-(7). Since SEIR reaction diffusion system (5)-(7) is a population model therefore negative values of susceptible, exposed and infected population is meaningless. Nonstandard finite difference method is a structural preserving numerical method which is developed by Mickens [16]. NSFD method is an important tool to solve ordinary and partial differential equations [9–11, 17, 18] as it preserves the properties possessed by continuous system.

2 Equilibrium Points

There are two steady states [15] of the system (5)-(7), disease-free and endemic steady state. Disease-free state is

$$(S_0, E_0, I_0) = (N, 0, 0) \tag{12}$$

and the endemic steady state is

$$(S_\star, E_\star, I_\star) = \left(\frac{N}{R_0}, \frac{\mu N}{\mu+\sigma}\left(1-\frac{1}{R_0}\right), \frac{\mu}{\beta}(R_0-1)\right), \tag{13}$$

where

$$R_0 = \frac{\sigma\beta N}{(\mu+\sigma)(\mu+\gamma)}, \text{when, } d_S = d_E = d_I = 0$$

R_0 is the reproductive and if $R_0 < 1$ then the system possesses disease free state and if $R_0 > 1$ then system possesses endemic state.

3 Stability of Equilibrium of the System

The system (5)-(7) is linearized about the equilibrium point $(S_\star, E_\star, I_\star)$ to have small perturbations $S(x,t)$,$E(x,t)$ and $I(x,t)$ as describe in [19]

$$\frac{\partial S}{\partial t} = a_{11}S_1 + a_{12}E_1 + a_{13}I_1 + d_S\frac{\partial^2 S}{\partial x^2}, \tag{14}$$

$$\frac{\partial E}{\partial t} = a_{21}S_1 + a_{22}E_1 + a_{23}I_1 + d_E\frac{\partial^2 E}{\partial x^2}, \tag{15}$$

$$\frac{\partial I}{\partial t} = a_{31}S_1 + a_{32}E_1 + a_{33}I_1 + d_I\frac{\partial^2 I}{\partial x^2}. \tag{16}$$

Suppose that the system (14)-(16) possesses Fourier series solution as mentioned in [19], then

$$S_1(x,t) = \sum_k S_k e^{\lambda t}cos(kx), \tag{17}$$

$$E_1(x,t) = \sum_k E_k e^{\lambda t}cos(kx), \tag{18}$$

$$I_1(x,t) = \sum_k I_k e^{\lambda t}cos(kx), \tag{19}$$

where k represents the wave number for the node n and $k = n\pi/2$, $(n = 1, 2, 3, \ldots)$. Replacing the values of $S_1(x,t)$, $E_1(x,t)$ and $I_1(x,t)$ in the system, it is transformed into

$$\sum_k (a_{11} - d_S k^2 - \lambda)S_k + \sum_k a_{12}E_k + \sum_k a_{13}I_k = 0, \tag{20}$$

$$\sum_k a_{21}S_k + \sum_k (a_{22} - d_E k^2 - \lambda)E_k + \sum_k a_{23}I_k = 0, \tag{21}$$

$$\sum_k a_{31}S_k + \sum_k a_{32}E_k + \sum_k (a_{33} - d_I k^2 - \lambda)I_k = 0. \tag{22}$$

The variational matrix $\mathcal{V}$ is for the equation (20)-(22) is

$$\mathcal{V} = \begin{pmatrix} a_{11} - d_S k^2 & a_{12} & a_{13} \\ a_{21} & a_{22} - d_E k^2 & a_{23} \\ a_{31} & a_{32} & a_{33} - d_I k^2 \end{pmatrix}, \tag{23}$$

where

$$a_{11} = -\mu - \beta I_\star,$$

$$
\begin{aligned}
a_{12} &= 0,\\
a_{13} &= -\beta S_\star,\\
a_{21} &= \beta I_\star,\\
a_{22} &= -\mu - \sigma,\\
a_{23} &= \beta S_\star,\\
a_{31} &= 0,\\
a_{32} &= \sigma,\\
a_{33} &= -\mu - \gamma.
\end{aligned}
$$

The characteristics equation for matrix $\mathcal{V}$ is

$$\lambda^3 + \eta_1\lambda^2 + \eta_2\lambda + \eta_3 = 0,$$

$$\eta_1 = -\left(a_{11} + a_{22} + a_{33} - d_S k^2 - d_E k^2 - d_I k^2\right),$$

$$
\begin{aligned}
\eta_2 = -(&a_{12}a_{21} - a_{11}a_{22} - a_{11}a_{33} + a_{13}a_{31} - a_{22}a_{33} + a_{23}a_{32} + a_{11}d_E k^2 + a_{11}d_I k^2\\
&+ a_{22}d_S k^2 + a_{33}d_S k^2 + a_{33}d_E k^2 - d_S d_E k^4 - d_S d_I k^4 - d_E d_I k^4),
\end{aligned}
$$

$$
\begin{aligned}
\eta_3 = &-a_{11}a_{22}a_{33} + a_{11}a_{23}a_{32} + a_{12}a_{21}a_{33} - a_{12}a_{23}a_{31} - a_{13}a_{21}a_{32} + a_{13}a_{22}a_{31} + a_{11}a_{22}d_E k^2\\
&- a_{12}a_{21}d_I k^2 + a_{11}a_{33}d_E k^2 - a_{13}a_{31}d_E k^2 + a_{22}a_{33}d_S k^2 - a_{23}a_{32}d_S k^2 - a_{11}d_E d_I k^4\\
&- a_{22}d_S d_I k^4 - a_{33}d_S d_E k^4 + d_S d_E d_I k^6.
\end{aligned}
$$

The Routh-Hurwitz stability criterion gives

$$\eta_1 > 0, \eta_3 > 0,$$

and

$$\eta_1\eta_2 - \eta_3 > 0.$$

Table 1: Values of parameters.

cases	β	σ	γ	μ
1	0.3×10^{-5}	45.6	73	0.02
2	0.5×10^{-4}	50	80	0.02
3	0.8×10^{-3}	58	85	0.02
4	0.9×10^{-3}	65	90	0.02
5	0.3×10^{-2}	77	99	0.02

Al-Showaikh et al. and Jansen et al. [15, 20]

4 Bifurcation Value of Transmission Coefficient β

The values of $S_\star$, $E_\star$ and $I_\star$ are substituted in $a_{11}, a_{22}, \cdots$, to obtain

$$a_{11} = -13688.874223\beta,$$

$$
\begin{aligned}
a_{12} &= 0,\\
a_{13} &= -73.052026,\\
a_{21} &= 13688.87422\beta - 0.02,\\
a_{22} &= -45.62,\\
a_{23} &= 73.052026,\\
a_{31} &= 0,\\
a_{32} &= 45.6,\\
a_{33} &= -73.02.
\end{aligned}
$$

The Routh-Hurwitz criterion for stability gives

$$\eta_1 = 13688.874223\beta + 118.790511 = f_1(\beta),$$

$$\eta_3 = 45626204.885735\beta - 66.387278 = f_2(\beta),$$

$$\eta_1\eta_2 - \eta_3 = 22236475224.061045\beta^2 + 147566036.674313\beta + 2032.880064 = f_3(\beta).$$

The equation $f_2(\beta) = 0$ provides the bifurcation value of β, which shifts the stability of the equilibrium point (i.e. from stable to unstable). The solution for $f_2(\beta)$ gives 0.000001455. The point of equilibrium is unstable for any value of β less than 0.000001455. Similarly, the bifurcation value of β for system without diffusion is 0.000001462. The equilibrium point of the system without diffusion is not stable for any value of β less than 0.000001462. It is concluded that bifurcation value of β with diffusion is less than bifurcation value of β without diffusion. In order to find the bifurcation value of β we consider case 1 in Table 1 and $d_S = 0.05$, $d_E = 0.01$, $d_I = 0.001$.

Table 2: Stability of Equilibrium.

cases	Point of Equilibrium	n	η_1	η_2	$\eta_1\eta_2 - \eta_3$	Stability
1	$(2.435 \times 10^7, 1.125 \times 10^4, 7022.67)$	1	1.1883×10^2	7.0491×10	2.4758×10^3	Stable
2	$(1.6010 \times 10^6, 1.9352 \times 10^4, 1.2092\times 10^4)$	1	130.8151	2.4215×10^3	1.0579×10^4	Stable
3	$(1.0631 \times 10^5, 1.7199 \times 10^4, 1.1733\times 10^4)$	1	152.5968	4.6323×10^4	1.6207×10^5	Stable
4	$(1.0005 \times 10^5, 1.5349 \times 10^4, 1.1083\times 10^4)$	1	165.1852	5.8407×10^4	2.0116×10^5	Stable
5	$(3.3015 \times 10^4, 1.2975 \times 10^4, 1.0090\times 10^4)$	1	206.4796	2.3093×10^5	8.7524×10^5	Stable

5 Numerical Methods

In order to handle the complexity and nonlinearity of the reaction-diffusion system (5)-(7), we implement two classical and two proposed nonstandard operator splitting finite difference methods. Operator splitting FD schemes are used by various authors to solve complex problems containing differential equations [19, 21–30]. Generally, the SEIR reaction-diffusion equations are split into two systems of equations. The nonlinear reaction steps

$$\frac{1}{2}\frac{\partial S}{\partial t} = \mu N - \mu S - \beta IS, \tag{24}$$

$$\frac{1}{2}\frac{\partial E}{\partial t} = \beta SI - (\mu + \sigma)E, \tag{25}$$

$$\frac{1}{2}\frac{\partial I}{\partial t} = \sigma E - (\mu + \gamma)I, \tag{26}$$

which are used for the first half step for time and the linear diffusion equation

$$\frac{1}{2}\frac{\partial S}{\partial t} = d_S\frac{\partial^2 S}{\partial x^2}, \tag{27}$$

$$\frac{1}{2}\frac{\partial E}{\partial t} = d_E\frac{\partial^2 E}{\partial x^2}, \tag{28}$$

$$\frac{1}{2}\frac{\partial I}{\partial t} = d_I\frac{\partial^2 I}{\partial x^2}, \tag{29}$$

which are implemented for the second half step of time. Firstly, we present forward Euler FD and Backward Euler schemes to solve the equations.

$$\bar{S}_i^{m+\frac{1}{2}} = S_i^m + \tau\left(\mu N - \mu S_i^m - \beta S_i^m I_i^m\right), \tag{30}$$

$$\bar{E}_i^{m+\frac{1}{2}} = E_i^m + \tau\left(\beta S_i^m I_i^m - (\mu + \sigma)E_i^m\right), \tag{31}$$

$$\bar{I}_i^{m+\frac{1}{2}} = I_i^m + \tau\left(\sigma E_i^m - (\mu + \gamma)I_i^m\right), \tag{32}$$

where S_i^m, E_i^m, I_i^m are the finite difference approximation values of S, E and I at $0 + ih, i = 0, 1, \ldots$ and time $m\tau, m = 0, 1, \ldots$ and $\bar{S}_i^{m+\frac{1}{2}}, \bar{E}_i^{m+\frac{1}{2}}$ and $\bar{I}_i^{m+\frac{1}{2}}$ reflect the representative values at the half time step. The procedure at first half time step is same for both forward Euler and Backward Euler FD schemes. At second half-time step, the procedure is different for both schemes. For forward Euler FD scheme, we use

$$S_i^{m+1} = \bar{S}_i^{m+\frac{1}{2}} + \lambda_1\left(\bar{S}_{i-1}^{m+\frac{1}{2}} - 2\bar{S}_i^{m+\frac{1}{2}} + \bar{S}_{i+1}^{m+\frac{1}{2}}\right), \tag{33}$$

$$E_i^{m+1} = \bar{E}_i^{m+\frac{1}{2}} + \lambda_2\left(\bar{E}_{i-1}^{m+\frac{1}{2}} - 2\bar{E}_i^{m+\frac{1}{2}} + \bar{E}_{i+1}^{m+\frac{1}{2}}\right), \tag{34}$$

$$I_i^{m+1} = \bar{I}_i^{m+\frac{1}{2}} + \lambda_3\left(\bar{I}_{i-1}^{m+\frac{1}{2}} - 2\bar{I}_i^{m+\frac{1}{2}} + \bar{I}_{i+1}^{m+\frac{1}{2}}\right). \tag{35}$$

The procedure for the backward Euler FD scheme is

$$-\lambda_1 S_{i-1}^{m+1} + (1 + 2\lambda_1)S_i^{m+1} - \lambda_1 S_{i-1}^{m+1} = \bar{S}_i^{m+\frac{1}{2}}, \tag{36}$$

$$-\lambda_2 E_{i-1}^{m+1} + (1 + 2\lambda_2)E_i^{m+1} - \lambda_2 E_{i-1}^{m+1} = \bar{E}_i^{m+\frac{1}{2}}, \tag{37}$$

$$-\lambda_3 I_{i-1}^{m+1} + (1 + 2\lambda_3)I_i^{m+1} - \lambda_3 I_{i-1}^{m+1} = \bar{I}_i^{m+\frac{1}{2}}. \tag{38}$$

Now we construct nonstandard FD schemes. By applying rules defined by Mickens [16], both nonstandard FD schemes at first half time step are

$$\bar{S}_i^{m+\frac{1}{2}} = \frac{S_i^m + \tau\mu N}{1 + \tau\mu + \tau\beta I_i^m}, \tag{39}$$

$$\bar{E}_i^{m+\frac{1}{2}} = \frac{E_i^m + \tau\beta S_i^m I_i^m}{1 + \tau(\mu + \sigma)}, \tag{40}$$

$$\bar{I}_i^{m+\frac{1}{2}} = \frac{I_i^m + \tau\sigma E_i^m}{1 + \tau(\mu + \gamma)}. \tag{41}$$

Positivity of the solution requires that if

$$S_i^m \geq 0, E_i^m \geq 0, I_i^m \geq 0, \text{ then } \bar{S}_i^{m+\frac{1}{2}} \geq 0, \bar{E}_i^{m+\frac{1}{2}} \geq 0, \bar{I}_i^{m+\frac{1}{2}} \geq 0. \tag{42}$$

The procedure is different for both NSFD operator splitting schemes at second half-time step. For explicit NSFD operator splitting scheme, we use

$$S_i^{m+1} = (1 - 2\lambda_1)\bar{S}_i^{m+\frac{1}{2}} + \lambda_1\left(\bar{S}_{i-1}^{m+\frac{1}{2}} + \bar{S}_{i+1}^{m+\frac{1}{2}}\right), \tag{43}$$

$$E_i^{m+1} = (1 - 2\lambda_2)\,\bar{E}_i^{m+\frac{1}{2}} + \lambda_2\left(\bar{E}_{i-1}^{m+\frac{1}{2}} + \bar{E}_{i+1}^{m+\frac{1}{2}}\right), \tag{44}$$

$$I_i^{m+1} = (1 - 2\lambda_3)\,\bar{I}_i^{m+\frac{1}{2}} + \lambda_3\left(\bar{I}_{i-1}^{m+\frac{1}{2}} + \bar{I}_{i+1}^{m+\frac{1}{2}}\right). \tag{45}$$

The procedure for the implicit NSFD operator splitting scheme at second half time step is

$$-\lambda_1 S_{i-1}^{m+1} + (1 + 2\lambda_1)\,S_i^{m+1} - \lambda_1 S_{i-1}^{m+1} = \bar{S}_i^{m+\frac{1}{2}}, \tag{46}$$

$$-\lambda_2 E_{i-1}^{m+1} + (1 + 2\lambda_2)\,E_i^{m+1} - \lambda_2 E_{i-1}^{m+1} = \bar{E}_i^{m+\frac{1}{2}}, \tag{47}$$

$$-\lambda_3 I_{i-1}^{m+1} + (1 + 2\lambda_3)\,I_i^{m+1} - \lambda_3 I_{i-1}^{m+1} = \bar{I}_i^{m+\frac{1}{2}}, \tag{48}$$

where

$$\lambda_1 = d_S\frac{\tau}{h^2}, \lambda_2 = d_E\frac{\tau}{h^2}, \lambda_3 = d_I\frac{\tau}{h^2}.$$

5.1 Accuracy and Stability of the Numerical Methods

In operator splitting methods, the stability and consistency depends on their split solutions [21, 22]. In all the above splitting methods, the reaction step is solved exactly and time derivative has $O(\tau)$ accuracy [21, 22]. Similarly, the diffusion step has $O(h^2)$ accuracy and the cumulative accuracy of all numerical schemes is first order in time and second order in space [21, 22]. For the stability, the reaction step is unconditionally stable in all cases as it is solved exactly [21, 22]. In forward Euler method operator splitting FD method and explicit NSFD operator splitting method (32)-(34), the stability region of diffusion step is

$$\lambda_i \le \frac{1}{2}, (i = 1, 2, 3). \tag{49}$$

In the backward Euler method operator splitting FD method and implicit NSFD operator splitting method, the diffusion step is unconditionally stable.

5.2 Positivity of NSFD methods

It can be observed that NSFD methods in reaction step (39)-(41) preserve the positivity property of the solution. For the diffusion step, explicit NSFD method (43)-(45) gives the positive solution if

$$1 - 2\lambda_i \ge 0, i = 1, 2, 3.$$

This implies that

$$\lambda_i \le \frac{1}{2}, (i = 1, 2, 3),$$

which is the stability condition (49) of NSFD method (39)-(41). This proves that the first NSFD method preserves the positivity property in its stability region. In order to prove the positivity of unconditionally stable implicit NSFD method (46)-(48), we use M-matrix theory [33].

5.2.1 Theorem [31, 32]

For any $h > 0$ and $\tau > 0$, the system (46)-(48) is positive, i.e. $S^m > 0$, $E^m > 0$ and $I^m > 0$ for all $m = 0, 1, 2\ldots$
Proof
The system (46)-(48) can be written as

$$AS^{m+1} = S^m, \tag{50}$$

$$BE^{m+1} = E^m, \tag{51}$$

$$CI^{m+1} = I^m, \tag{52}$$

where A, B and C are the square matrices

$$A = \begin{pmatrix} a_3 & a_1 & 0 & \cdots & \cdots & \cdots & 0 \\ a_2 & a_3 & a_2 & \ddots & & & \vdots \\ 0 & a_2 & a_3 & a_2 & \ddots & & \vdots \\ \vdots & \ddots & \ddots & \ddots & \ddots & \ddots & \vdots \\ \vdots & & \ddots & \ddots & \ddots & \ddots & \vdots \\ \vdots & & & \ddots & a_2 & a_3 & a_2 \\ 0 & \cdots & \cdots & \cdots & 0 & a_1 & a_3 \end{pmatrix}, \tag{53}$$

$$B = \begin{pmatrix} b_3 & b_1 & 0 & \cdots & \cdots & \cdots & 0 \\ b_2 & b_3 & b_2 & \ddots & & & \vdots \\ 0 & b_2 & b_3 & b_2 & \ddots & & \vdots \\ \vdots & \ddots & \ddots & \ddots & \ddots & \ddots & \vdots \\ \vdots & & \ddots & \ddots & \ddots & \ddots & \vdots \\ \vdots & & & \ddots & b_2 & b_3 & b_2 \\ 0 & \cdots & \cdots & \cdots & 0 & b_1 & b_3 \end{pmatrix}, \tag{54}$$

and

$$C = \begin{pmatrix} c_3 & c_1 & 0 & \cdots & \cdots & \cdots & 0 \\ c_2 & c_3 & c_2 & \ddots & & & \vdots \\ 0 & c_2 & c_3 & c_2 & \ddots & & \vdots \\ \vdots & \ddots & \ddots & \ddots & \ddots & \ddots & \vdots \\ \vdots & & \ddots & \ddots & \ddots & \ddots & \vdots \\ \vdots & & & \ddots & c_2 & c_3 & c_2 \\ 0 & \cdots & \cdots & \cdots & 0 & c_1 & c_3 \end{pmatrix}. \tag{55}$$

The off-diagonal entries of A are $a_1 = -2\lambda_1$, $a_2 = -\lambda_1$ and $a_3 = 1 + 2\lambda_1$. The off-diagonal entries of B are $b_1 = -2\lambda_1$, $b_2 = -\lambda_1$and diagonal entries are $b_3 = 1 + 2\lambda_2$. The off-diagonal entries of C are $c_1 = -2\lambda_3$, $c_2 = -\lambda_3$and diagonal entries are $c_3 = 1 + 2\lambda_3$. Thus A, B and C are M-matrices. Hence equation (50), (51) and (52) become

$$S^{m+1} = A^{-1}S^m, \tag{56}$$

$$E^{m+1} = B^{-1}E^m, \tag{57}$$

$$I^{m+1} = C^{-1}I^m. \tag{58}$$

If we consider that $S^m > 0, E^m > 0$ and $I^m > 0$, then from the property of M-matrix and (56)-(58) we get $S^{m+1} > 0, E^{m+1} > 0$ and $I^{m+1} > 0$. So by the induction, the theorem is proved.
It follows from Theorem 5.2.1 that implicit NSFD operator splitting scheme preserve positivity property unconditionally.

6 Numerical Experiment

In this section, we perform a numerical experiment for all the methods at both equilibrium points. For the numerical test, the following values of parameters are used for disease-free equilibrium [15, 20]

$$N = 5 \times 10^7, \mu = 0.02, \sigma = 45.6, \gamma = 73, \beta = 0.1 \times 10^{-5}. \tag{59}$$

For endemic equilibrium points, the following parametric values are used [15, 20]

$$N = 5 \times 10^7, \mu = 0.02, \sigma = 45.6, \gamma = 73, \beta = 0.3 \times 10^{-5}. \tag{60}$$

In this experiment we take $d_S = 0.05, d_E = 0.01, d_I = 0.001$. The initial conditions for the system (5)-(7) are

$$S(x,0) = \begin{cases} 12500000x & \text{if } 0 \le x < 0.5 \\ 12500000\,(1-x) & \text{if } 0.5 \le x \le 1 \end{cases}, \tag{61}$$

$$E(x,0) = \begin{cases} 50000x & \text{if } 0 \le x < 0.5 \\ 50000\,(1-x) & \text{if } 0.5 \le x \le 1 \end{cases}, \tag{62}$$

$$I(x,0) = \begin{cases} 30000x & \text{if } 0 \le x < 0.5 \\ 30000\,(1-x) & \text{if } 0.5 \le x \le 1 \end{cases}. \tag{63}$$

Now the graphs of all the schemes at disease free equilibrium point is presented. First of all we show the graphs of Forward Euler operator splitting FD scheme.

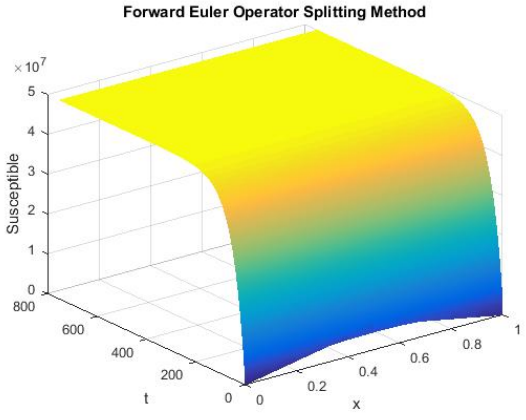

Figure 1: Mesh graph of Susceptible Individuals for DFE

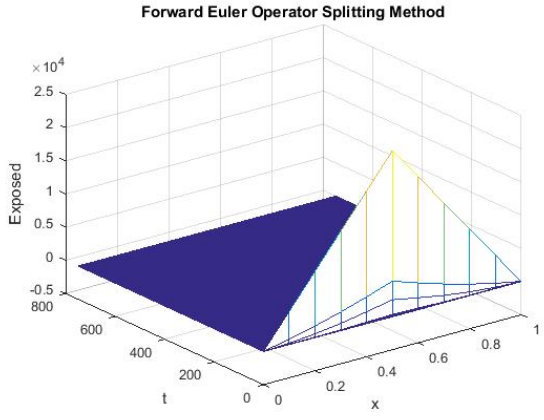

Figure 2: Mesh graph of Exposed Individuals for DFE

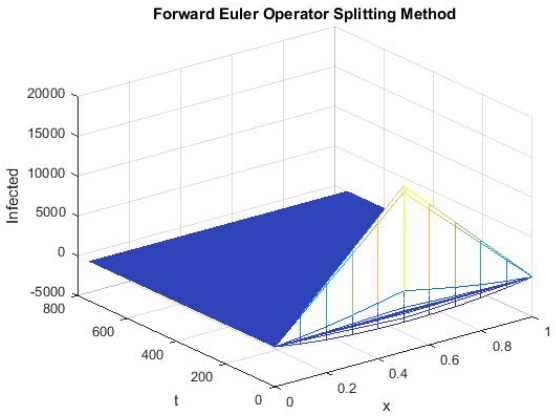

Figure 3: Mesh graph of Infected Individuals for DFE

The figures 1-3 indicate the graphs of disease free equilibrium using forward Euler operator splitting FD scheme at $h = 0.1$ and $\lambda_1 = 0.09375, \lambda_2 = 0.01875$ and $\lambda_3 = 0.001875$. Figure 2 and figure 3 show that forward Euler operator splitting FD scheme fails to preserve the positivity property.

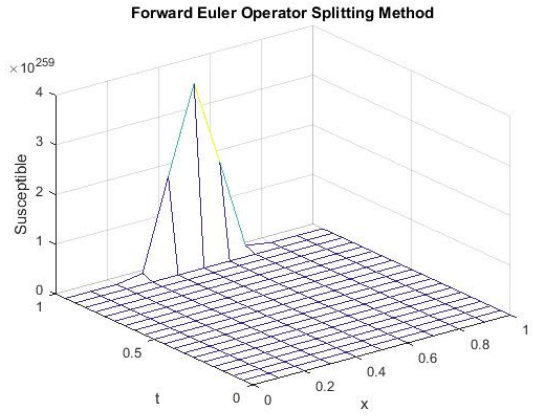

Figure 4: Mesh graph of Susceptible Individuals for EE

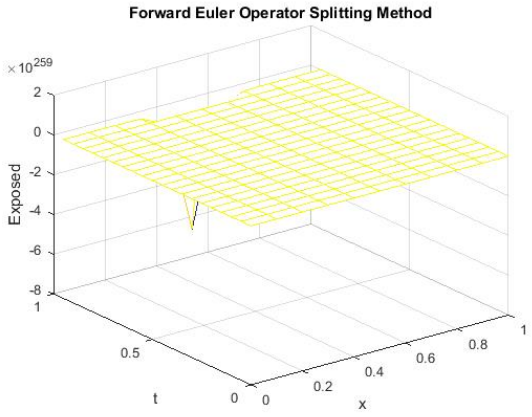

Figure 5: Mesh graph of Exposed Individuals for EE

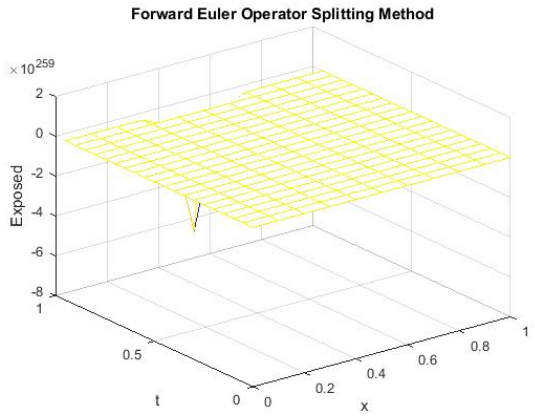

Figure 6: Mesh graph of Infected Individuals for EE

The figures 4-6 represent the mesh graphs of susceptible, exposed and infected individuals using forward Euler explicit operator splitting FD scheme at $h = 0.1$ and $\lambda_1 = 0.25, \lambda_2 = 0.05$ and $\lambda_3 = 0.005$. It can be seen that all the graphs in figures 4-6 show overflow and divergence. Remember that these are the graphs at endemic equilibrium point. Forward Euler explicit operator splitting FD scheme fails to converge to the endemic equilibrium point. Secondly we present the simulation of backward Euler implicit operator splitting FD scheme.

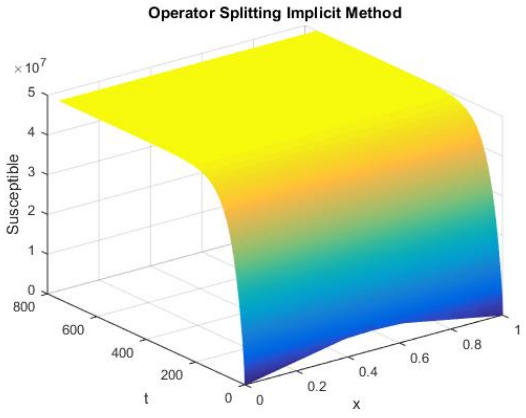

Figure 7: Mesh graph of Susceptible Individuals for DFE

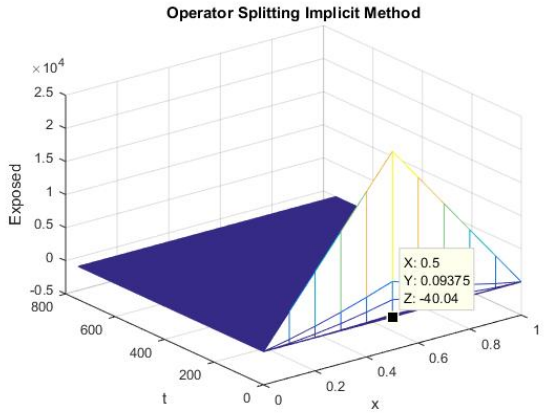

Figure 8: Mesh graph of Exposed Individuals for DFE

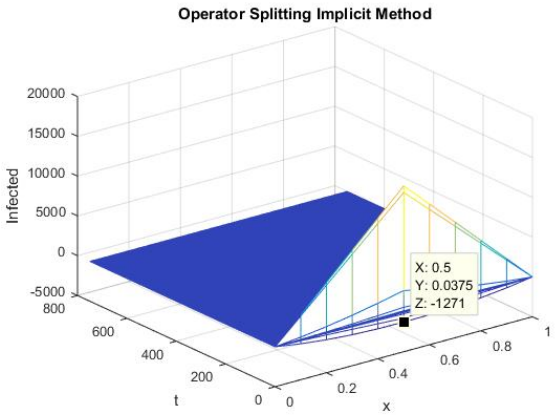

Figure 9: Mesh graph of Infected Individuals for DFE

The figures 7-9 reflect the graphs of disease free equilibrium using backward Euler implicit operator splitting FD scheme at $h = 0.1$ and $\lambda_1 = 0.09375, \lambda_2 = 0.01875$ and $\lambda_3 = 0.001875$. Figure 8 and figure 9 show that backward Euler implicit operator splitting FD scheme also fails to preserve the positivity property.

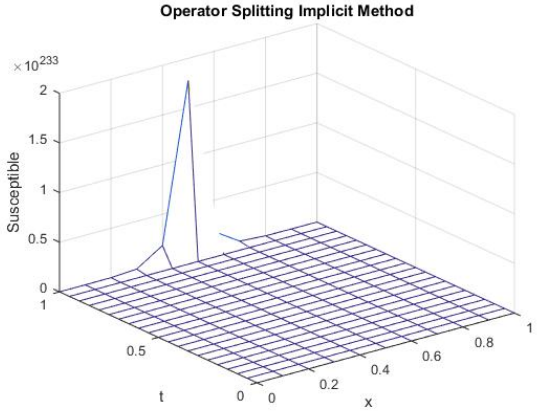

Figure 10: Mesh graph of Susceptible Individuals for EE

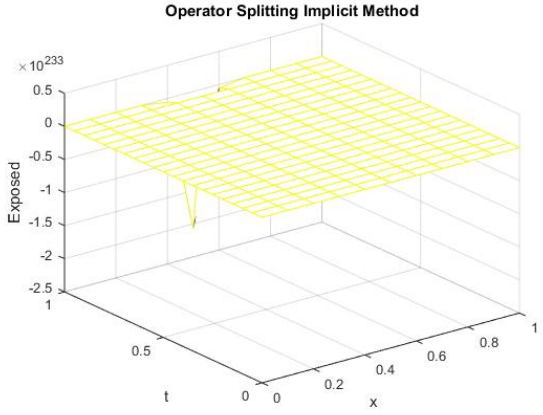

Figure 11: Mesh graph of Exposed Individuals for EE

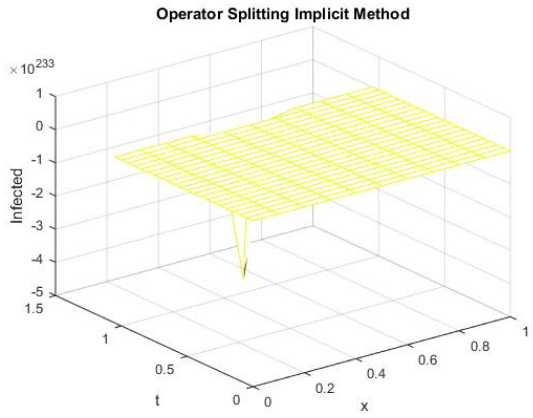

Figure 12: Mesh graph of Infected Individuals for EE

The figures 10-12 represent the mesh graphs of susceptible, exposed and infected individuals using backward Euler implicit operator splitting FD scheme at $h = 0.1$ and $\lambda_1 = 0.25, \lambda_2 = 0.05$ and $\lambda_3 = 0.005$. It can be seen that all the graphs in figures 10-12 show overflow and divergence. Remember that these are the graphs at endemic equilibrium point. Backward Euler implicit operator splitting FD scheme fails to converge to the endemic equilibrium point. Thirdly, the graphs of susceptible, exposed and infected population at disease free and endemic equilibrium point using nonstandard operator splitting explicit FD method are presented.

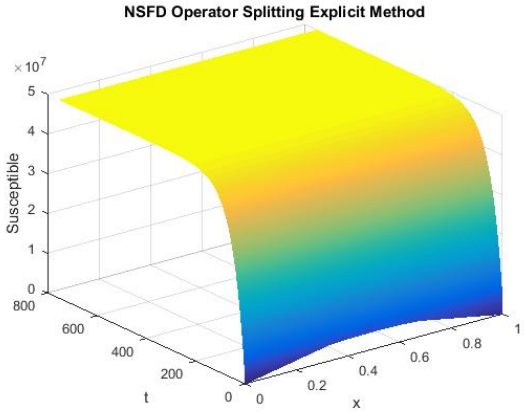

Figure 13: Mesh graph of Susceptible Individuals for DFE

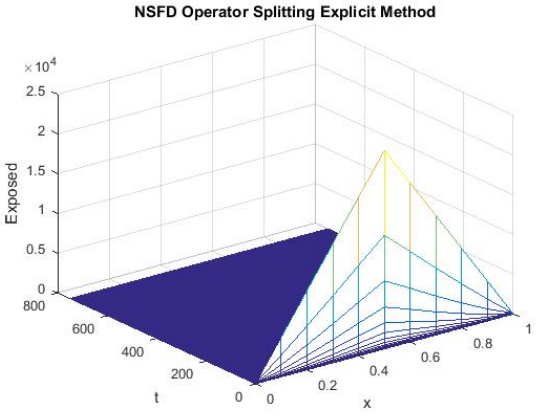

Figure 14: Mesh graph of Exposed Individuals for DFE

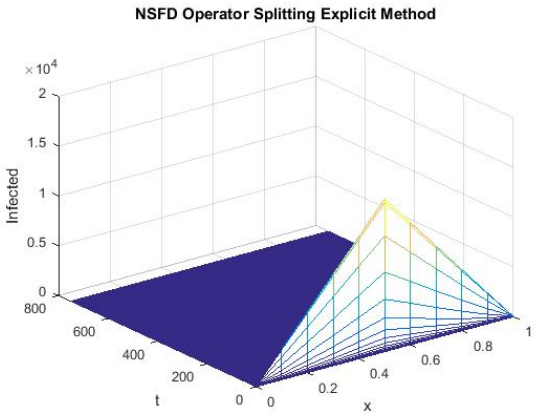

Figure 15: Mesh graph of Infected Individuals for DFE

The figures 13-15 reflect the graphs of disease free equilibrium using NSFD explicit operator splitting scheme at $h = 0.1$ and $\lambda_1 = 0.09375, \lambda_2 = 0.01875$ and $\lambda_3 = 0.001875$. Graphs clearly show that NSFD operator splitting explicit scheme preserves the positivity property and converges to the disease free equilibrium point (S_0, E_0, I_0).

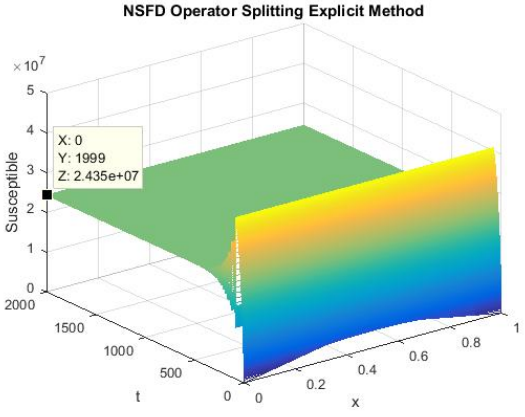

Figure 16: Mesh graph of Susceptible Individuals for EE

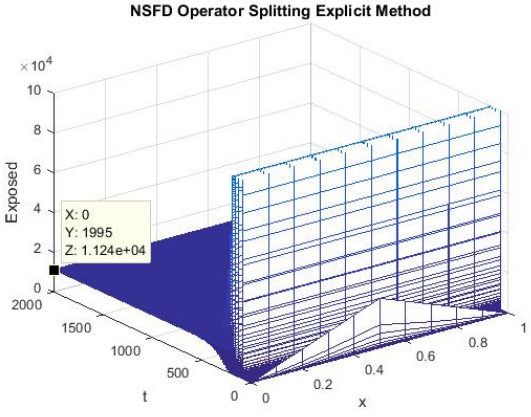

Figure 17: Mesh graph of Exposed Individuals for EE

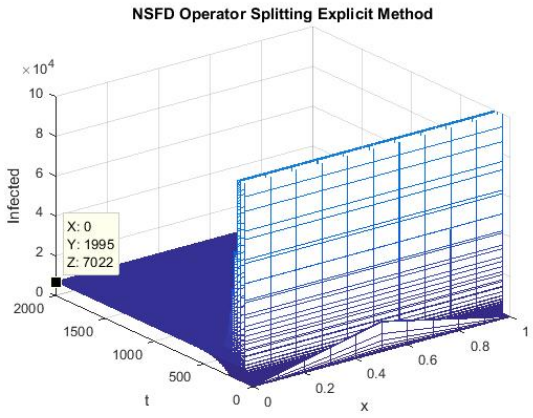

Figure 18: Mesh graph of Infected Individuals for EE

The figures 16-18 represent the graphs of endemic equilibrium point for susceptible, exposed and infected individuals using NSFD operator splitting explicit scheme at $h = 0.1$ and $\lambda_1 = 0.25, \lambda_2 = 0.05$ and $\lambda_3 = 0.005$. Graphs show that NSFD operator splitting explicit scheme preserves the positivity property and converges to the endemic equilibrium point $(S_\star, E_\star, I_\star)$. At the end, we present the simulations using NSFD operator splitting implicit method.

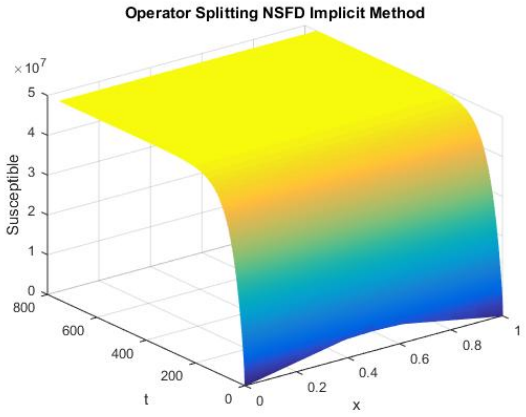

Figure 19: Mesh graph of Susceptible Individuals for DFE

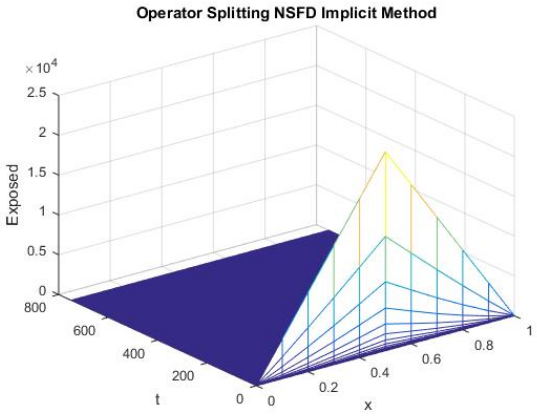

Figure 20: Mesh graph of Exposed Individuals for DFE

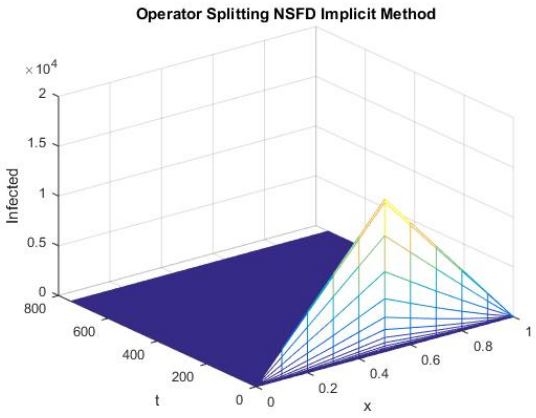

Figure 21: Mesh graph of Infected Individuals for DFE

Figures 19-21 reflect the graphs of disease free equilibrium using NSFD operator splitting implicit scheme at $h = 0.1$ and $\lambda_1 = 0.09375, \lambda_2 = 0.01875$ and $\lambda_3 = 0.001875$. Graphs clearly show that NSFD operator splitting implicit scheme preserves the positivity property and converges to the disease free equilibrium point (S_0, E_0, I_0).

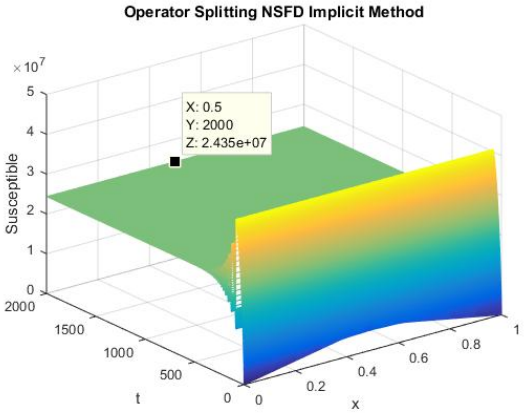

Figure 22: Mesh graph of Susceptible Individuals for EE

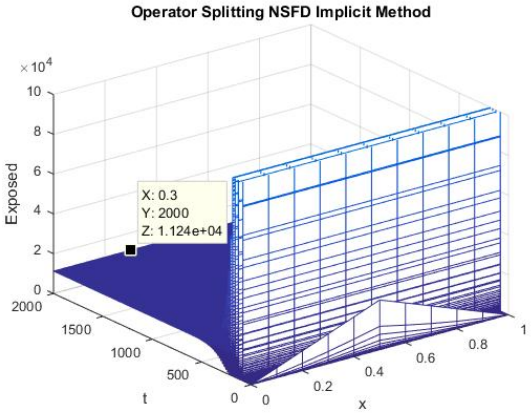

Figure 23: Mesh graph of Exposed Individuals for EE

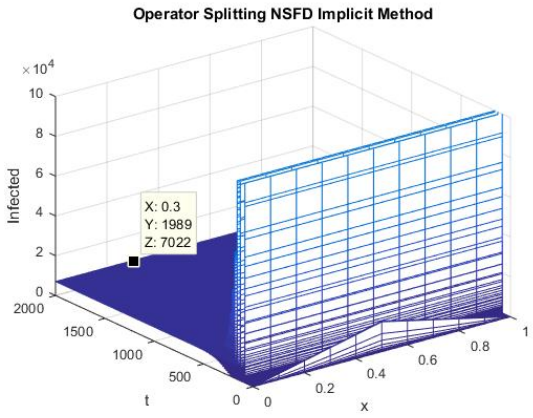

Figure 24: Mesh graph of Infected Individuals for EE

The figures 22-24 represent the graphs of endemic equilibrium point for susceptible, exposed and infected individuals using NSFD operator splitting implicit scheme at $h = 0.1$ and $\lambda_1 = 0.25, \lambda_2 = 0.05$ and $\lambda_3 = 0.005$. Graphs show that NSFD operator splitting implicit method preserves the positivity property and converges to the endemic equilibrium point $(S_\star, E_\star, I_\star)$.

7 Conclusion

In this work, we developed two positivity preserving nonstandard finite difference schemes which did not bring contrived chaos. The proposed NSFD schemes are operator splitting FD schemes. We showed that classical operator splitting FD schemes bring the contrived chaos which lead to the numerical instabilities. We also give the stability analysis of SEIR reaction-diffusion system and find out the bifurcation value of transmission coefficient with the help of Routh-Hurwitz criteria. The proposed NSFD operator splitting schemes should prove to be of value in the solution of nonlinear continuous dynamical systems. Our future plane includes the construction of NSFD operator splitting techniques for hidden attractors in continuous dynamical systems [34–37].

Acknowledgement: We are thankful to the reviewer for spending his time and giving his valuable suggestions to improve this manuscript.

References

[1] Hamer, W. H., Epidemic disease in England, Lancet, (1906), 1 , 733–739.
[2] Kaninda, A.V., Legros, D., Jataou, I.M., Malfait, P., Maisonneuve, M., Paquet, C., Moren, A., Measles vaccine Effectiveness in Standard and Early Immunization Strategies, Niger. Pediatr. Infect., (1998), 17 ,1034–1039.
[3] Hethcote, H.W., Optimal ages for vaccination for Measles, Math. Biosci, (1989), 89, 29-52.
[4] Bakare, E. A., Adekunle, Y. A., Kadiri, K. O., Modeling and Simulation of the dynamics of the transmission of Measles, International journal of Computer Trends and Technology, (2012), 3(1), 174-177.
[5] Okosun, K. O., Mukamuri, M., Makinde, D. O., Global stability analysis and control of leptospirosis, Open Math., (2016), 14, 567–585.
[6] Ahmed, N., Rafiq, M., Rehman, M. A., Iqbal, M. S., Ali, M. Numerical modelling of three dimensional Brusselator reaction diffusion system, AIP Advances, (2019), 9, 015205
[7] Fatima, U., Ali, M., Ahmed, N., Rafiq, M., Numerical modeling of susceptible latent breaking-out quarantine computer virus epidemic dynamics, Heliyon, (2018), 4, e00631.

[8] Twizell, E.H., Wang, Y., Price, W.G., Chaos-free numerical solutions of reaction-diffusion equations, Proc.R. Soc. Lond. A, (1991), 430, 541-576.
[9] Rafiq, M., Numerical Modeling of Infectious Diseases Dynamics, (PhD thesis), Lahore: University of Engineering and Technology.
[10] Ahmed, N., Jawaz, M., Rafiq, M., Rehman, M. A., Ali, M., Ahmad, M. O., Numerical Treatment of an Epidemic Model with Spatial Diffusion, J. Appl. Environ. Biol. Sci., (2018), 8(6), 17-29.
[11] Ahmed, N., Shahid, N., Iqbal, Z., Jawaz, M., Rafiq, M., Tahira. S. S., Ahmad, M. O., Numerical Modeling of SEIQV Epidemic Model with Saturated Incidence Rate, J. Appl. Environ. Biol. Sci., (2018), 8(4).
[12] Ahmed, N., Rafiq, M., Rehman, M. A., Ali, M., Ahmad, M. O., Numerical Modeling of SEIR Measles Dynamics with Diffusion, Communications in Mathematics and Applications, (2018), 9(3), 315–326,
[13] Chinviriyasit, S., Chinviriyasit, W., Numerical modeling of SIR epidemic model with diffusion, Appl. Math. Comp., (2010), 216, 395–409.
[14] Fernández, Francisco M., On some approximate methods for nonlinear models, Applied Mathematics and Computation, (2009), 215, 168–174.
[15] Al-Showaikh, F., Twizell, E., One-dimensional measles dynamics, Appl. Math. Comput., (2004), 152, 169-194.
[16] Mickens, R. E., Nonstandard Finite Difference Models of Differential Equations, (1994), World Scientific.
[17] Mickens, R. E., A nonstandard finite difference scheme for a Fisher PDE having nonlinear diffusion, Computer and Mathematics with Application, (2003), 45, 429-436.
[18] Mickens, R. E., A nonstandard finite difference scheme for an advection-reaction equation, J. Diff. Eq. Appl., (2004), 10, 1307-1312.
[19] Chakrabrty, A., Singh, M., Lucy, B., Ridland, P., Predator-prey model with pry- taxis and diffusion, Math. Comput. Modeling, (2007), 46, 482-498.
[20] Jansen, H., Twizell, E. H., An unconditionally convergent discretization of the SEIR model, MATH COMPUT SIMULAT., (2002), 58, 147-158.
[21] Harwood, R. C. Operator splitting method and applications for semilinear parabolic partial differential equations (Ph.D. dissertation), (2011), Pullman: Dept. Math., Washington State Univ.
[22] Harwood, R. C., Manoranjan, V. S., Edwards, D. B., Lead-acid battery model under discharge with a fast splitting method, IEEE Trans. Energy Convers., (2011), 26 (4), 1109-1117.
[23] Yanenko, N. N., The Method of Fractional Steps (Springer-Verlag, 1971).
[24] Zharnitsky, V., Averaging for split-step scheme, Nonlinearity, (2003), 16, 1359-1366.
[25] Ansarizadeh, F., Singh, M., Richards, D., Modelling of tumor cells regression in response to chemotherapeutic treatment, Applied Mathematical Modeling, (2017), 48, 96-112 .
[26] Naheed, A., Singh, M., Lucy, D., Effect of Treatment on Transmission Dynamics of SARS Epidemic, J. Infect. Non. Infect. Dis., (2016).
[27] Naheed, A., A Study of Spatio-Temporal Spread of Infectious Disease:SARS, (Ph.D. thesis), (2015), , Australia: Swinburne University of Technology.
[28] Naheed, A., Singh, M., Lucy, D., Numerical study of SARS epidemic model with the inclusion of diffusion in the system, Applied Mathematics and computation, (2014), 229, 480-498.
[29] Samsuzzoha, Md., A Study on numerical solutions of epidemic models , (2012), (Ph.D. thesis), Australia: Swinburne University of Technology.
[30] Wang, H. Q., Numerical studies on the split-step finite difference method for nonlinear Schrödinger equations, Applied Mathematics and Computation, (2005), 170, 17-35
[31] Manna, K., Chakrabarty, S. P., Global stability and a non-standard finite difference scheme for a diffusion driven HBV model with capsids, J. Differ. Equ. Appl., (2015), 21, 918-933.
[32] Qin, W., Wang, L., Ding, X., A non-standard finite difference method for a hepatitis B virus infection model with spatial diffusion, J. Differ. Equ. Appl., (2014), 20(12), 1641–1651.
[33] Fujimoto, T., Ranade, R., Two characterizations of inverse–positive matrices: The Hawkins–Simon condition and the Le Chatelier–Braun principle, Electron. J. Linear Algebra, (2004), 11, 59–65.
[34] Wei, Z.C., Moroz, I., Sprott, J.C., Akgul, A., Zhang, W., Hidden hyperchaos and electronic circuit application in a 5D self-exciting homopolar disc dynamo, Chaos, (2017), 27, 033101.
[35] Wei, Z.C., Moroz, I., Sprott, J.C., Wang, Z., Zhang , W., Detecting hidden chaotic regions and complex dynamics in the self-exciting homopolar disc dynamo, Int. J. Bifurc. Chaos, (2017), 27, 1730008 .
[36] Wei, Z., Yu, P., Zhang, W., Minghui Yao, Study of hidden attractors, multiple limit cycles from Hopf bifurcation and boundedness of motion in the generalized hyperchaotic Rabinovich system, Nonlinear Dyn., (2015), 10.1007/s11071-015-2144-8.
[37] Wei, Z., Zhua B., Yanga, J., Perc, M., Slavinec, M., Bifurcation analysis of two disc dynamos with viscous friction and multiple time delays, Applied Mathematics and Computation, (2019), 347, 265–281